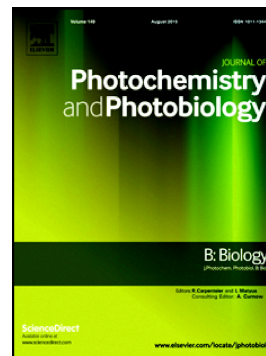


Journal Pre-proof

Sensitized photo-oxidation of gadusol species mediated by singlet oxygen

Dalila Elisabet Orallo, Nayla Jimena Lores, Ernesto Maximiliano Arbeloa, Sonia Graciela Bertolotti, Maria Sandra Churio



PII: S1011-1344(20)30528-5

DOI: <https://doi.org/10.1016/j.jphotobiol.2020.112078>

Reference: JPB 112078

To appear in: *Journal of Photochemistry & Photobiology, B: Biology*

Received date: 5 August 2020

Revised date: 20 October 2020

Accepted date: 31 October 2020

Please cite this article as: D.E. Orallo, N.J. Lores, E.M. Arbeloa, et al., Sensitized photo-oxidation of gadusol species mediated by singlet oxygen, *Journal of Photochemistry & Photobiology, B: Biology* (2020), <https://doi.org/10.1016/j.jphotobiol.2020.112078>

This is a PDF file of an article that has undergone enhancements after acceptance, such as the addition of a cover page and metadata, and formatting for readability, but it is not yet the definitive version of record. This version will undergo additional copyediting, typesetting and review before it is published in its final form, but we are providing this version to give early visibility of the article. Please note that, during the production process, errors may be discovered which could affect the content, and all legal disclaimers that apply to the journal pertain.

© 2020 Published by Elsevier.

Sensitized photo-oxidation of gadusol species mediated by singlet oxygen

Dalila Elisabet Orallo^{1,2}, Nayla Jimena Lores^{1,3}, Ernesto Maximiliano Arbeloa^{4,5}, Sonia Graciela Bertolotti^{4,5} and María Sandra Churio*^{1,2}

¹ Departamento de Química y Bioquímica, Facultad de Ciencias Exactas y Naturales, Universidad Nacional de Mar del Plata (UNMDP), Funes 3350, B7602AYL - Mar del Plata, Argentina.

² Instituto de Física de Mar del Plata (IFIMAR), Consejo Nacional de Investigaciones Científicas y Técnicas (CONICET), Funes 3350, B7602AYL - Mar del Plata, Argentina.

³ División Polímeros Biomédicos. Instituto de Investigaciones en Ciencia y Tecnología de Materiales (INTEMA) UNMDP-CONICET. Av. Juan B. Justo 4302. B7608FDQ. Mar del Plata, Argentina.

⁴ Departamento de Química, Facultad de Ciencias Exactas, Físico-Químicas y Naturales, Universidad Nacional de Río Cuarto, Campus Universitario. km 601, X5804ALH - Río Cuarto, Argentina.

⁵ Instituto de Investigaciones en Tecnologías Energéticas y Materiales Avanzados (IITEMA) UNRC-CONICET.

* schurio@mdp.edu.ar (María Sandra Churio)

ABSTRACT

Gadusols are efficient nature UV sunscreens with antioxidant capacity. The kinetics of the quenching reactions of singlet oxygen $O_2(^1\Delta_g)$ by gadusol species was evaluated in aqueous solution as well as in the presence of direct charged micelles. Time-resolved phosphorescence detection of $O_2(^1\Delta_g)$ indicated that gadusolate, the main species under biological pH, is a more efficient quencher than the enol form with a rate constant of *ca.* $1.3 \times 10^8 \text{ L mol}^{-1} \text{ s}^{-1}$. The deactivation proceeds *via* a collisional mechanism with clear dominance of chemical pathways, according to the rates of gadusol and oxygen consumptions, and typical photooxidation quantum yields of *ca.* 7%. The relative contributions of the chemical and physical quenching steps were not affected by the presence of anionic or cationic micelles emulating simple pseudo-biological environments. The products of the photo-oxidative quenching support a type II mechanism initiated by the addition of $O_2(^1\Delta_g)$ to the C-C double bond of gadusolate. These results point to the relevance of considering the role of sacrifice antioxidant along with the UV-screening function for gadusol, particularly in the context of potential biotechnological applications of this natural molecule.

Keywords UV photoprotection, quenching kinetics, natural antioxidant, direct micelles.

Abbreviations GADH (Gadusol), GAD (Gadusolate), RB (Rose Bengal), TRP (*L*-Tryptophan), PN (Phenalenone)

1. INTRODUCTION

Gadusol (3,5,6-trihydroxy-5-hydroxymethyl-2-methoxycyclohex-2-en-1-one) and the analogous 6-deoxygadusol (3,5-dihydroxy-5-hydroxymethyl-2-methoxycyclohex-2-en-1-one) are structural- and biosynthetically related to the natural UV-absorbing compounds mycosporine and mycosporine-like amino acids (MAAs) [1-3]. Sunscreening and antioxidant functions have been frequently suggested for this group of secondary metabolites, broadly distributed among fresh water, marine and terrestrial organisms [4-6].

The absorption spectrum of gadusol in aqueous solution shifts its maximum from 268 nm ($\epsilon = 12400 \text{ L mol}^{-1} \text{ cm}^{-1}$) to 296 nm ($\epsilon = 21800 \text{ L mol}^{-1} \text{ cm}^{-1}$) on going from acidic to neutral pHs (see Fig. 1b) [7,8]. These bands are respectively assigned to the enol (GADH) and the enolate (GAD) forms of the compound ($pK_a = 4.2$) (see Fig. 1a) [8, 9]. MAAs however absorb intensively at longer wavelengths within the transition zone between the UV-A and the UV-B portions of the solar spectrum. On this basis it has been proposed that gadusols may have played an important role as UV/C screens in the early stages of phototrophic life that developed under an O_2 -depleted atmosphere [1, 10, 11]. Experimental and theoretical studies support this hypothesis by confirming the high photostability of the metabolite in aqueous solution under physiological pH and its rapid deactivation through efficient dissipation of light energy as heat [7, 12]. Evolution of gadusols to MAAs *via* amine condensation reactions may have fulfilled the increasing requirements of protection against UVA and photooxidative stress that followed the accumulation of oxygen in the atmosphere [10, 13].

The UV-screening properties of gadusol have received particular attention in reference to potential roles in marine organisms [14, 15]. Bok *et al.* have identified the presence of MAAs and a gadusol-related compound in the visual system of the stomatopod species

Neogonodactylus oerstedii (mantis shrimp) [14]. The UV-specific optical filtering of the compounds in the crystalline cones seems to provide spectral tuning allowing unique polychromatic UV vision in *N. oerstedii* [14]. MAAs and gadusols also occur in association with soluble proteins in fish lenses from various species [4, 16, 17]. Although the functional significance of these complexes is not fully understood, it is suggested that the UV absorbing pigments may protect the retina from harmful radiation in shallow water fish or also improve visual acuity by avoiding shorter wavelengths that are responsible for chromatic aberration and scattering [18]. Furthermore, reactivity against UV-induced radical species should not be discarded as an additional mechanism of protective action within ocular tissues [19].

Besides, the high concentration of gadusol in the roes of marine fish suggests a functional role in embryonic development, probably based on the UV-photoprotective and the antioxidant abilities of this molecule [15–20]. The metabolite was initially thought to be acquired by fish through diet but it was recently found that the biosynthetic genes are present in vertebrates too [21]. This is lately exploited through genetical engineering to form hybrid structures of gadusol and mycosporine-like amino acids, conceived as a platform for the design and production of novel sunscreens [22].

The interest on unravelling the mechanistic basis of the photoprotective potential of these ubiquitous molecules is currently increasing along with the urgent demands of new ideas for the design of the next generation of sunscreens [23, 24]. In this context, complementation of the UV filter capacity with antioxidant action is relevant for development of more efficient and safer photoprotectors [25, 26]. The antioxidant capacity of gadusols has been evaluated through different methods. The phosphatidylcholine peroxidation inhibition-assay yielded larger activity for deoxygadusol than for the oxo-MAA mycosporine-glycine [27]. The

determination of the oxygen radical absorbance capacity (ORAC) and the test based on the 2,2'-azinobis (3-ethylbenzothiazoline-6-sulphonic acid) diammonium salt (ABTS) confirmed that the enolate form, GAD, is comparable to ascorbic acid towards reductive reactions with radicals although its ability to break chain reactions carried by peroxy radicals is stronger [28]. The affinity of GAD for reducing photoexcited species has been considered as an extra contribution to the antioxidant capacity of the metabolite [7]. Suh *et al* assessed the deactivation of singlet oxygen molecules ($O_2(^1\Delta_g)$) by deoxygadusol through competitive inhibition of rubrene oxidation [29]. The study yielded a quenching rate constant larger than those for the amino acids histidine and methionine. However, the experiments were carried out in chloroform/methanol solvent mixtures which hardly reflect the physiological conditions. In addition, the technique used by the authors provides a total quenching rate constant, k_t , without discerning the mechanism by which $O_2(^1\Delta_g)$ is removed by deoxygadusol.

A deeper characterization of the interaction of gadusol species with singlet oxygen in aqueous media is necessary to better visualize their participation as protectors against photooxidative stress in reproductive and vision systems of marine biota species, and their potential applications as natural antioxidant and photoprotective additives for the elaboration of food and cosmetics products. In this context we herein report on the total and reactive quenching rate constants of singlet oxygen by gadusol species in aqueous solutions. We also explored the kinetics of the reaction in the presence of micelles prepared with ionic surfactants in order to compare the efficiency of the photodynamic event in simple models of biomembranes.

2. MATERIALS AND METHODS

2.1. Sample preparation

Gadusol was extracted from fish roes of Argentinian sandperch (*Pseudoperca semifasciata*) as described elsewhere [28]. Solutions of gadusol in D₂O (Aldrich, 99.9%) were prepared by redissolving concentrated aqueous solutions of the metabolite in this solvent. The extracts were concentrated under vacuum and the D₂O was added under Ar atmosphere.

SDS (Sigma-Aldrich, > 99%) or CTAC (Sigma-Aldrich, 25% solution) were used for preparing micellar solutions. CTAC was previously purified by evaporation to dryness and recrystallization from a 50% ethanol-acetone mixture. The critical micellar concentration (CMC) values were verified by conductimetry and the results, SDS: $8.0 \times 10^{-3} \text{ mol L}^{-1}$ and CTAC: $1.4 \times 10^{-3} \text{ mol L}^{-1}$, were in full agreement with previous reports [30]. The solid surfactant was dissolved in tridistilled water or D₂O to achieve 0.10 mol L^{-1} concentration and buffering. Aliquots of a concentrated GAD solution in the same solvent were added into the micellar solution.

The pH (or pD) in the acidic range (between 2.4 and 5) was fixed with phosphate buffer solutions prepared with H₃PO₄ (Cicaelli, P.A.) and KH₂PO₄ (Sigma, $\geq 99.0\%$) at 0.03 mol L^{-1} final concentration. The pD values were calculated by the expression $\text{pD} = \text{pH} + 0.4$. Otherwise indicated, the homogeneous and tensioactive solutions under neutral conditions were regulated with 0.05 mol L^{-1} tris[hydroxymethyl]amino-methane Trizma® base/Trizma® HCl (Sigma, reagent grade) for pH (pD) 8.

Singlet oxygen was generated in air-saturated solutions by photosensitization with Rose Bengal (RB) or phenalenone (PN). Both sensitizers were purchased from Aldrich, with 95% and 97% purity respectively, and used as received. The absorbance of the sensitizer at the irradiation wavelengths was *ca.* 0.4 for RB (530 or 532 nm) and 0.5 for PN (355 nm).

2.2. Time-resolved phosphorescence detection (TRPD)

Laser irradiation with *ca.* 18 ns-pulse width was carried out with a Nd:YAG laser (Spectron Laser SL400) at 355 nm (PN in homogeneous solutions), 532 nm (RB in homogeneous or micellar D₂O solutions), and 266 nm (direct irradiation of gadusol). PN was chosen as an alternative sensitizer in the experiments at pD 2.4 due to the bleaching of RB at pH < 3.

The phosphorescence emission from singlet oxygen after the excitation laser pulse was registered at 1270 nm with a Ge amplified detector (Judson J16/8Sp). The emission previously passed through cut-off (< 1000 nm) and interference (1270 nm) filters. The detector readily followed the emission from about 4-6 μ s after the laser pulse. The output was coupled to a digital oscilloscope and to a personal computer for the signal processing. The signals from 10 laser pulses were averaged and the obtained trace was fitted to monoexponential functions of time, characterized by τ_{Δ} , the exponential time constant assigned to singlet oxygen lifetime.

2.3. Reactive quenching studies

The reactive quenching of singlet oxygen was evaluated by following the decrease of the substrate and/or oxygen concentrations under stationary irradiation, at room temperature and continuous stirring.

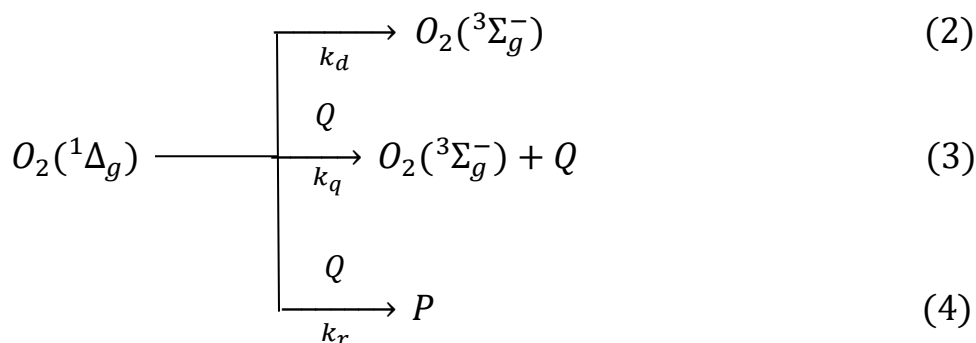
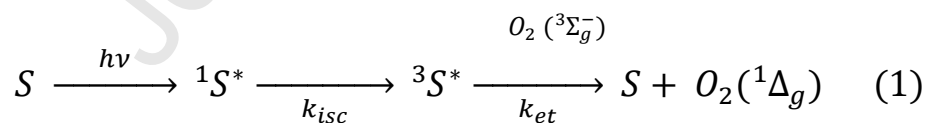
Singlet oxygen was generated by photosensitization with RB at 530-nm LED light (Philips). *L*-Tryptophan (TRP, SigmaUltra, 98%) in Trizma® base/Trizma® HCl buffer at pH 8 was taken as the reference ($k_r = 3.2 \times 10^7 \text{ L mol}^{-1} \text{ s}^{-1}$) [31]. GAD consumption was determined by UV-absorption spectrophotometry at 296 nm as a function of the irradiation time. Analogously, the decrease in GADH concentration was evaluated at 268 nm; in this case the irradiation experiment was carried out at pH 5 in 0.1 mol L⁻¹ phosphate buffer. The changes in TRP

concentration were followed at 280 nm. The rates of consumption determined spectrophotometrically were consistent with the results from the evaluation by HPLC analysis, carried out preliminarily as control experiments (Lichrocart® TC-C18, 5 µm, 4 mm d.i. x 25 cm column and gradient elution from 100% Trizma® base/Trizma® HCl buffer at pH 8; flow rate 1 mL min⁻¹). Further control experiments with RB solutions in the absence of the quenchers verified that no modification of the absorption spectrum of the sensitizer takes place under the same conditions (concentration, light source and irradiation time). Similarly, no variation in the absorption spectra was observed in the absence of irradiation for the solutions containing both RB and any of the quenchers, thus dark interactions with the sensitizer were discarded.

Oxygen concentration was monitored during irradiation with a specific electrode (Orion 97-08) coupled to a hermetically sealed cell containing the solution under study.

2.4. Evaluation of the quenching rate constants

The following set of reactions summarizes the general scheme involved in the generation and deactivation of $O_2(^1\Delta_g)$ that guided the experimental evaluations of the kinetic constants.



This mechanism represents a type II process, according to Foote's classification [32, 33], where a sensitizer (denoted as S) is excited to a triplet state and transfers energy to ground state oxygen, generating $O_2(^1\Delta_g)$ (eqn.1). The excited oxygen species can decay by collision with solvent molecules (eqn.2) and/or physically or chemically interact with a quencher Q (eqns. 3 and 4). In eqn. 4, P stands for the product(s) of the chemical reaction between $O_2(^1\Delta_g)$ and the quencher molecule Q . Thus, the total quenching constant k_t represents the sum of k_r and k_q , the rate constants for chemical (reactive) and physical quenching, respectively.

The total quenching rate constants k_t were here estimated from the analysis of $O_2(^1\Delta_g)$ emission decays obtained by TRPD as a function of the quencher molar concentration $[Q]$. Considering that τ_Δ^0 represents singlet oxygen lifetime in the absence of Q , the lifetimes in the presence of Q , τ_Δ , were fitted to the Stern-Volmer expression: $(\tau_\Delta)^{-1} = (\tau_\Delta^0)^{-1} + k_t[Q]$.

The reactive quenching constants k_r were assessed from the stationary photosensitization experiments described in the previous section by comparison of the quenching rates for each substrate against the standard quencher TRP [34]. The kinetic analysis for continuous irradiation of the singlet oxygen sensitizer S in the presence of the reactive quencher Q leads to the quencher depletion rate described by eqn.5:

$$-\frac{d[Q]}{dt} = k_r[O_2(^1\Delta_g)]_{ss}[Q] = k_r'[Q] \quad (5)$$

The expression assumes that a steady state singlet oxygen concentration $[O_2(^1\Delta_g)]_{ss}$ is attained and that no reaction between Q and S takes place. Thus, the pseudo-first order rate

constant, k_r' , is given by the product between k_r and the steady state singlet oxygen concentration. Integration of eqn. 5 predicts the linearity of a plot of $\ln([Q]/[Q]_0)$ vs. t , with k_r' as the slope.

For identical experimental conditions such as light intensity and S concentration, $[O_2(^1\Delta_g)]_{ss}$ remains unchanged, and the ratio of the slopes of the first order plots for the consumption of the quencher and the reference substrate yields the ratio of their respective k_r values. The reactive quenching constant for Q was derived from this ratio and the reference value of the reactive quenching constant for TRP [31, 34].

Molecular oxygen is consumed in reaction (4), thus k_r can be also estimated from the evaluation of oxygen uptake during photoirradiation. Recalling that Q is in great excess with respect to the concentration of singlet oxygen, [Q] can be considered nearly constant during the earlier reaction times. The rate law is now expressed in terms of singlet oxygen disappearance as a pseudo-first order process where k_r'' represents the pseudo-rate constant including [Q], as shown in eqn.6.

$$-\frac{d[O_2(^1\Delta_g)]}{dt} = k_r[O_2(^1\Delta_g)][Q] = k_r''[O_2(^1\Delta_g)] \quad (6)$$

Upon integration of eqn. 6, a plot of $\ln([O_2]/[O_2]_0)$ vs. t is expected to be lineal. The ratio of the slopes of the lines for equivalent experiments, with matched concentrations of the quencher and the reference TRP, should afford the reactive quenching constant k_r for Q relative to that one for TRP.

2.5. Quencher distribution in micellar media

The partition of GAD in the micellar solutions was evaluated by two kinds of experiments. In first place, aliquots of 3.0×10^{-3} mol L⁻¹ GAD in 0.10 mol L⁻¹ surfactant (SDS or CTAC) were respectively placed in ultracentrifugal filter devices of 0.5 mL capacity with 10,000 Da cut off

membrane (Ultrafree-MC Amicon-Bioseparations, Millipore). The samples were centrifuged at 6000 rpm for 40 min (Eppendorf 5402 centrifugation unit). Free GAD in the ultrafiltrate was determined by UV-vis absorption spectrophotometry. Control experiments, carried out in the absence of the surfactants, showed that no capture of GAD by the membrane occurred. All the experiments were performed at 20°C and repeated at least twice.

On the other hand, aqueous solutions of GAD $3.4 \times 10^{-5} \text{ mol L}^{-1}$ were mixed with the same volumes of *n*-octanol and stirred. The biphasic systems were kept for 48 h at room temperature in the dark. Then, aliquots from both the aqueous and the organic phases were separately analyzed by spectrophotometry in order to determine the presence of the metabolite.

2.6. Mass spectrometry analysis

Identification of the photoproducts of the quenching of $O_2(^1\Delta_g)$ by GAD was carried out by liquid chromatography coupled to mass spectrometry (LC/MS). Aqueous solutions containing GAD and RB at pH 8 were analyzed. Two samples were irradiated with the LED at 530 nm up to 20 % and 100% conversion of GAD, respectively evaluated by UV absorbance. A control sample was kept in the dark before the analysis. The LC/MS system was equipped with an HPLC chromatograph (HPLC Waters Aquity H-class) and a triple quadrupole mass spectrometer (Xevo TQS- Micro). HPLC analyses were performed using an Aquity BEH-C18 (1.7 μm ; 2.1 x 100 mm) column and gradient elution from 100% formic acid $1 \times 10^{-2} \text{ mol L}^{-1}$ /water to 100% formic acid $1 \times 10^{-2} \text{ mol L}^{-1}$ /methanol at a flow rate of 0.25 mL min^{-1} . The mass spectrometer was operated in both positive and negative ion modes. Nitrogen served as auxiliary, collision gas, and nebulizer gas. The flow rate of nitrogen was 500 L min^{-1} , temperature 400°C and the voltage in the capillary was set at 2 kV. The spectra were obtained by using an equipment collision cell with argon at a

pressure of 4×10^{-3} mbar.

3. RESULTS

3.1. Generation of $O_2(^1\Delta_g)$ by gadusolate

No phosphorescent signal was observed, within the instrumental detection limits of the TRPD, when 2×10^{-5} mol L⁻¹ gadusol in D₂O was irradiated at 266 nm. Under the neutral pD conditions of the experiment, GAD was the dominant species with *ca.* 0.3 absorbance at 266 nm. The control experiment with RB in D₂O and similar absorbance at the irradiation wavelength (532 nm) showed the characteristic emission of $O_2(^1\Delta_g)$ at 1270 nm. The phosphorescence decayed monoexponentially with $\tau_{\Delta} = 66$ μ s, in good agreement with the reported values [35].

3.2. Quenching of $O_2(^1\Delta_g)$ by gadusol species in aqueous solution

The effect of GADH concentration on τ_{Δ} was evaluated by TRPD in D₂O. Under the acidic conditions of the experiments (pD 2.4), the addition of a concentrated aliquot of aqueous GADH (final concentration 1.3×10^{-3} mol L⁻¹) did not modify the decay of the $O_2(^1\Delta_g)$ emission in comparison with a blank experiment in which the same volume of aqueous buffer was introduced into the PN/D₂O solution (traces not shown). Lifetimes obtained in the absence and in presence of GADH differed only within ± 1 μ s. Thus, within the experimental uncertainty, τ_{Δ} kept unaltered, this setting an upper limit to the total quenching constant by GADH of $k_t \leq (1.8 \pm 0.8) \times 10^5$ L mol⁻¹s⁻¹.

In contrast, singlet oxygen phosphorescence decayed faster in the presence of GAD (pD 8.0) (see Supporting Information A). The signals fitted to monoexponential functions of

time in all the cases and revealed that τ_{Δ} reduces to *ca.* 50% its value without quenchers in the presence of 1.4×10^{-4} mol L⁻¹ GAD. The effect can be described in terms of the Stern-Volmer behavior, *i.e.* the dependence of τ_{Δ}^{-1} with substrate or quencher concentration is linear (Fig. 2). Similar results were obtained for solutions under pD 5. The slopes of the lines provide the total quenching rate constants k_t summarized in Table 1. Some examples of the phosphorescence decays are shown in Supporting Information B.

The reactive quenching of $O_2(^1\Delta_g)$ by gadusol species was evaluated on the basis of eqn. 5 in terms of the quencher consumption in steady-state photolysis experiments with RB by following the quencher absorbance as a function of time. The results at pH 5 show that each of the two absorption maxima (268 nm and 296 nm, respectively assigned to the forms GADH and GAD involved in the acid-base equilibrium of gadusol (Fig. 1 a)) decays with a distinctive rate (see Supporting Information D). The change in time of the peak absorbances leads to the pseudo-first order plots shown in Fig. 3 a. The lower slope of the logarithmic plot for the absorbance at 268 nm reflects the consumption of GAD due to the shift of its equilibrium with GADH, the only reactive form involved in the reactive quenching of $O_2(^1\Delta_g)$.

Table 1 summarizes the results for the reactive quenching constant by GAD. An effective kinetic constant of $(0.93 \pm 0.11) \times 10^8$ L mol⁻¹ s⁻¹ is estimated from the time evolution of the 296 nm-absorbance band maxima in the experiment at pH 5. On the other hand, the evaluation of GAD consumption at pH 8, yields a value of $k_r = (1.05 \pm 0.19) \times 10^8$ L mol⁻¹ s⁻¹ (see the time evolution of the absorption spectra in Supporting Information E) Both results are coincident, within the experimental uncertainty, affording an averaged reactive quenching constant of $k_r = (0.99 \pm 0.22) \times 10^8$ L mol⁻¹ s⁻¹.

Additionally, the time evolution of oxygen uptake was determined for the quenching by GAD at pH 8 and compared to the kinetics of TRP depletion, taken as the reference. According to eqn. 6, the linear regression of the plots of molecular oxygen concentration vs. irradiation time (Fig. 3b) allowed the estimation of the reactive quenching constant for GAD $k_r = (0.80 \pm 0.10) \times 10^8 \text{ L mol}^{-1} \text{ s}^{-1}$ reported in Table 1.

3.3. Quenching of $O_2(^1\Delta_g)$ by gadusolate in the presence of micelles

The distribution of GAD, as the physiologically relevant form of the metabolite, was assessed in micellar solutions of ionic surfactants: SDS and CTAC. The concentration of GAD decreased up to 3% of its initial value in any of the micellar solutions after ultrafiltration. This change is within the experimental error related to the absorbance determinations. Consistently, no presence of gadusol species could be detected, within the experimental uncertainties, in the organic phase of the *n*-octanol/water mixtures. Both results support a negligible partition of gadusol species in the hydrophobic microphases associated to the direct micelles.

The rate constants for the total quenching of $O_2(^1\Delta_g)$ by GAD in SDS or CTAC micelles were determined by TRPD in D_2O buffered at pD 8 and 0.10 mol L^{-1} surfactant. The phosphorescence lifetimes, τ_Δ , were visibly shortened by GAD concentration in both micellar solutions (examples of the phosphorescence decays are shown in Supporting Information C). The data followed the Stern-Volmer dependence (see Fig. 2 for SDS solution, as an example). The linear regression afforded good fits to straight lines, with slopes yielding the total rate constants k_t reported in Table 1: $(1.09 \pm 0.13) \times 10^8 \text{ L mol}^{-1} \text{ s}^{-1}$ for SDS, and $(1.17 \pm 0.11) \times 10^8 \text{ L mol}^{-1} \text{ s}^{-1}$ for CTAC.

The rate constants for the reactive quenching of $O_2(^1\Delta_g)$ by GAD in the presence of SDS and CTAC micelles were determined by the decrease of quencher concentration. The quenching by TRP in buffered aqueous solution (pH 8) was taken as the reference process. The pseudo-first order plots for GAD in the presence of each surfactant and in aqueous solution are compared in Fig. 4. The slopes of the straight lines yielded respectively the apparent rate constants $k_{r,app}$ in the micellar solutions, according to the integrated form of eqn. 5: $(0.99 \pm 0.12) \times 10^8 \text{ L mol}^{-1} \text{ s}^{-1}$ for CTAC, and $(1.02 \pm 0.11) \times 10^8 \text{ L mol}^{-1} \text{ s}^{-1}$ for SDS (Table 1).

3.4. Analysis of the products of the reactive quenching of $O_2(^1\Delta_g)$ by gadusolate

The LC/MS analysis carried out on the aqueous mixture of GAD and RB before irradiation yielded the signals corresponding to the molecular ion of the metabolite as the $[M-H]^-$ species at m/z 203. The chromatograms for the irradiated solutions revealed additional signals at m/z 235 in the negative mode that may correspond to the addition of O_2 to GAD (molecular weight of 236 g mol^{-1}). Other signals at m/z 191 in the negative mode (192 g mol^{-1} molecular weight) and at m/z 119 in the positive mode (118 g mol^{-1} molecular weight) can be explained by degradation products. The abundance of the ions m/z 191 and 119 increased with decreasing the intensity of the signal assigned to GAD. Supporting Information F to H shows the LC chromatograms. The MS fragmentation spectra corresponding to the signals at m/z 203, 235 and 119, are displayed in Supporting Information I to K.

The intensity of the peak corresponding to the molecular ion m/z 203 was consistent with the extents of the reaction (20% and 100%) in the analyzed samples, as estimated by the UV absorbance assigned to GAD.

4. DISCUSSION

The direct irradiation experiment at 266 nm in D₂O confirms that photosensitized generation of $O_2(^1\Delta_g)$ by GAD can be disregarded. This is well explained by the negligible intersystem crossing quantum yield for photoexcited GAD, that rules out its potential contribution as sensitizer in the reaction sequence of eqn. 1 [7]. Instead, ground state gadusol species are able to quench $O_2(^1\Delta_g)$ in aqueous solutions. Particularly, the quenching experiments at neutral pH evidence the efficient deactivation of $O_2(^1\Delta_g)$ by GAD. The quenching follows a collisional mechanism, as deduced from the Stern-Volmer behavior (Fig. 2). The process is represented by the reactions in eqns. 3 and 4, with Q denoting GAD. The order of magnitude of the total quenching rate constant, $k_t = 1.27 \times 10^8 \text{ L mol}^{-1} \text{ s}^{-1}$ (see Table 1) is comparable to those for natural antioxidants such as ascorbic acid in H₂O ($6.8 \times 10^8 \text{ L mol}^{-1} \text{ s}^{-1}$) [36] or in D₂O: acetonitrile mixtures ($3.1 \times 10^8 \text{ L mol}^{-1} \text{ s}^{-1}$) [37] and α -tocopherol in methanol: chloroform solvent mixtures ($1.5 \times 10^8 \text{ L mol}^{-1} \text{ s}^{-1}$) [38]. The result is also in line with the quenching rates evaluated for the structural-related compounds deoxygadusol ($5.4 \times 10^7 \text{ L mol}^{-1} \text{ s}^{-1}$), mycosporine-glycine ($6.7 \times 10^7 \text{ L mol}^{-1} \text{ s}^{-1}$), both in methanol:chloroform mixtures [29], and mycosporine-glutaminol-glucoside ($5.9 \times 10^7 \text{ L mol}^{-1} \text{ s}^{-1}$) in D₂O [39].

No quenching ability was detected for the enol form GADH in aqueous solution (pD 2.4). This sets an upper limit to the rate constant for the total quenching by this species estimated as $(1.8 \pm 0.8) \times 10^5 \text{ L mol}^{-1} \text{ s}^{-1}$, *i.e.* around 700-times slower than that one for GAD. Similarly, strong pH-dependences in the $O_2(^1\Delta_g)$ quenching rates by ascorbic acid, histidine and N-acetyl tyrosine ethyl ester have been reported and associated to the higher reactivity of the deprotonated forms of the quenchers [36, 37]. The same effect seems to explain the *ca.*

22% drop in the value of k_t in aqueous solution at pD 5 in comparison with pD 8 (Fig. 2, Table 1). Since equilibrium concentrations of the enol (GADH) and enolate (GAD) forms are expected to be comparable under pH values close to the pK_a [9], the presence of GADH in the acidic solution lowers the overall reactivity in comparison with neutral solutions that contain the anionic form GAD almost exclusively.

The results for the reactive quenching constant, k_r , follow the same trend as the total quenching constants, k_t , amounting *ca.* $1.0 \times 10^8 \text{ L mol}^{-1} \text{ s}^{-1}$ for GAD (Table 1). Moreover, the ratio k_r/k_t for GAD is close to 1, within the experimental uncertainties, pointing to the dominant chemical nature of the quenching process. Besides, comparison of the magnitudes of k_r for GAD obtained by substrate depletion and by oxygen uptake (Fig. 3, Table 1) supports the 1:1 stoichiometry assigned to the quenching reaction in eqn. 4.

In view of these results, gadusol species could be considered as sacrifice antioxidants, enabling the question about their possible roles in pro-oxidant pathways in aerobic life. The efficiency of the degradation reaction by $O_2(^1\Delta_g)$ can be described for GAD, as the biologically relevant species, in terms of the photooxidation quantum yield, Φ_r . This parameter is calculated from eqn. 7 for a given GAD concentration [40].

$$\Phi_r = \frac{\Phi_{\Delta} k_r [GAD]}{(\tau_{\Delta}^0)^{-1} + k_r [GAD]} \quad (7)$$

In the last expression, Φ_{Δ} stands for the quantum yield of $O_2(^1\Delta_g)$ production by the sensitizer and the inverse of τ_{Δ}^0 represents the specific rate of all the events that lead to the deactivation of $O_2(^1\Delta_g)$ in the absence of GAD (eqns. 2-4). Thus, Φ_r amounts 7% for $[GAD] = 2 \times 10^{-4} \text{ mol L}^{-1}$ in aqueous solution, RB as sensitizer with $\Phi_{\Delta} = 0.8$ [41], $\tau_{\Delta}^0 = 4 \mu\text{s}$ [42), k_r and k_t from

representative values at pH 8 (Table 1), and assuming that the total quenching constant in D₂O is equivalent to that one in H₂O. This result compares well with the photooxidation quantum yield reported for ascorbate, estimated in *ca.* 2% [36].

The electrophilic character of $O_2(^1\Delta_g)$ suggests that the reactivity towards gadusols might be related to the presence of unsaturated groups in the molecule [43]. Then, it seems reasonable that $O_2(^1\Delta_g)$ adds to the double bond in the carbon ring, as a first event before subsequent rearrangement. This in turn explains the larger reactivity of GAD in comparison to GADH, since the deprotonation of the OH group in the β -carbon increases the nucleophilic character of the double bond *via* conjugation effects.

The identification of the photooxidation products was achieved by LC/MS analysis. The chromatographic peak at the retention time of GAD vanished, while new signals attributable to the products could be detected. The molecular weight of 236 g mol⁻¹ (m/z 235, negative mode) is assigned to the intermediate I₁ that arises from the intramolecular rearrangement of the addition of a $O_2(^1\Delta_g)$ to the double bond in the cyclic structure of GAD (Fig.5). This indicates a type II photooxidation process governing the reaction between GAD and $O_2(^1\Delta_g)$. The molecular weight of 192 g mol⁻¹ (m/z 191, negative mode) is proposed to correspond to the intermediate compound I₂ produced from the decarboxylation of I₁. Analogous pathways were proposed in the reaction mechanism for pterin-photosensitized oxidation of TRP by $O_2(^1\Delta_g)$ reported by Thomas *et al.* [44]. Two final photoproducts: methyl 3-hydrox-2-oxopropanoate (P₁) and 1-hydroxyacetone (P₂) are postulated to originate from the cleavage and rearrangement of I₂, as described in the scheme of Fig. 5. Photoproduct P₁ was identified experimentally through the signal for m/z 119 in the positive mode (molecular weight of 118 g mol⁻¹). The low molecular weight of product P₂ probably prevented it to be

detected in either of the two modes used. Recalling that gadusol has been extracted from fish roes, it is interesting to note that P_1 could be metabolized by the cytochrome P450 in fish [45]. This system comprises the enzymes that are necessary to convert P_1 to pyruvic acid or to conjugating it with glucuronic acid for its excretion from the organism.

In view of the latter results, we considered that a complex biological environment may condition the extent of the sensitized photooxidation of GAD by affecting the balance between reactive and physical deactivation of singlet oxygen. Higher degrees of self-protection against $O_2(^1\Delta_g)$ in micellar systems have been already reported for the singlet molecular oxygen mediated photooxidation of amino acids such as tyrosine and related compounds. This behaviour was visualized through lower ratios of $k_{r,app}/k_{t,app}$ that favour the physical quenching [46]. Therefore, aiming at an initial step in the extrapolation of the results to biological environments, we examined the quenching of $O_2(^1\Delta_g)$ by GAD in the presence of charged surfactants over their respective CMC in aqueous solution.

The results from ultrafiltration and *n*-octanol/water partition determinations support that GAD species are preferentially placed in the aqueous phase, rather than in the hydrophobic interior of the direct micelles. However, general electrostatic interactions between GAD and the charged micelles may induce a preferential location of the anionic form of the metabolite in the outer interfacial zone of cationic CTAC micelles, as already observed for the related metabolites MAAs [47]. Thus, alterations of the environment for the quenching event in this kind of microheterogeneous systems were preliminarily expected [48, 49]. The slopes of the linear plots for micellar solutions in Figs. 2 and 4 evidence just subtle effects of the presence of any of the direct charged micelles, anionic SDS or cationic CTAC ones, on the rates of total and reactive $O_2(^1\Delta_g)$ quenchings in comparison with plain aqueous solution. For

the evaluation of quenching kinetics in micellar systems it is assumed that the diffusion of $O_2(^1\Delta_g)$ molecules in and out of the micelles is rapid enough so that their dynamics can be considered independent of the site where they were generated by photosensitization [50]. On this basis, apparent rate constants $k_{t,app}$ and $k_{r,app}$ were obtained for the microheterogeneous media with values around $1 \times 10^8 \text{ L mol}^{-1} \text{ s}^{-1}$, respectively. Within the experimental uncertainties, these constants amount similar to the rest of the values reported in Table 1 for GAD in aqueous solution at pH(pD) 8. It is concluded that the relative contribution of the chemical quenching to the global quenching process is not affected by the presence of charged micelles. Still, larger influences in the extent of the quenching of GAD in membranes should not be discarded, in analogy to those reported for the physical quenching of $O_2(^1\Delta_g)$ by azide anion in more complex microheterogeneous environments [51].

5. CONCLUSIONS

This study assesses for the first time the kinetics of the photo-oxidation of gadusol species by $O_2(^1\Delta_g)$ in aqueous solution as well as in the presence of direct charged micelles. The results support a collisional mechanism of quenching. GAD, the anionic species dominating the equilibrium distribution around neutral pH, presents a larger quenching efficiency in comparison to GADH, probably due to the enhanced nucleophilic character of the molecule. The products identified for the photo-oxidation support a type II mechanism initiated by the addition of $O_2(^1\Delta_g)$ to the C-C double bond.

Although the relative contributions of the chemical and physical deactivations in the quenching mechanisms are not affected by the presence of direct charged micelles which emulate simple pseudo-biological environments, stronger effects in more complex

environments should not be discarded. Further exploration of these effects is relevant to control of the reactivity under ambient atmospheres in the context of potential biotechnological applications of the metabolite.

Finally, the prevailing chemical nature of the quenching mechanisms suggests that GAD may play the role of a sacrifice antioxidant along with the UV-screening function in living organisms and raises the question about the interplay and balance with other reactive species under physiological conditions.

ACKNOWLEDGMENTS

This study was funded by Universidad Nacional de Mar del Plata (15/E920-EXA962/20), ANPCyT (PICT 2016-1672), and Universidad Nacional de Río Cuarto. The authors are grateful to J. I. Carreto and M. Carignan (INIDEP) for their kind assistance in the ultrafiltration experiments, and to J. F. Espinosa (Inst. Fares-Taie) for technical support in the LC/MS determinations. N. J. Lores thanks UNMDP for her student fellowship 2013.

REFERENCES

- [1] J. M. Shick, V. C. Dunlap, Mycosporines-like amino acids and related gadusols: Biosynthesis, accumulation, and UV-protective functions in aquatic organisms, *Annu. Rev. Physiol.* 64 (2002) 223–262.
- [2] J. I. Carreto, M. O. Carignan, Mycosporine-like amino acids: Relevant secondary metabolites, Chemical and ecological aspects, *Mar. Drugs.* 9 (2011) 387–446.
- [3] E. P. Balskus, C. T. Walsh, The genetic and molecular basis for sunscreen biosynthesis in cyanobacteria, *Science*, 329 (2010) 1653–1656.

- [4] W. M. Bandaranayake, Mycosporines. Are they nature's sunscreens?, *Nat. Prod. Rep.* 15 (1998) 159–172.
- [5] W. C. Dunlap, J. M. Shick, Y. Yamamoto, in: *Free radicals in Chemistry, Biology and Medicine*, T. Yoshikawa, S. Toyokuni, Y. Yamamoto, Y. Naito (Eds.), Ultraviolet (UV) protection in marine organisms. Sunscreens, oxidative stress and antioxidants, OICA Int. London, 2000, pp. 201-214.
- [6] R. Losantos, D. Sampedro, M. S. Churio, Photochemistry and photophysics of mycosporine-like amino acids and gadusols, nature's ultraviolet screens, *Pure Appl. Chem.* 87 (2015) 979–996.
- [7] E. M. Arbeloa, S. G. Bertolotti, M. S. Churio, Photophysics and reductive quenching reactivity of gadusol in solution, *Photochem. Photobiol. Sci.* 10 (2011) 133–142.
- [8] P. T. Grant, P. A. Plack, R. H. Thomson, Gadusol, a metabolite from fish eggs, *Tetrahedron Lett.* 21 (1980) 4043–4044.
- [9] P. A. Plack, N. W. Fraser, P. T. Grant, C. Middleton, A. I. Mitchell, R. H. Thomson. Gadusol, an enolic derivative of cyclohexane-1,3-dione present in the roes of cod and other marine fish. *Biochem. J.* 195 (1981) 741–747.
- [10] F. Garcia-Pichel, Solar ultraviolet and evolutionary history of cyanobacteria, *Origins Life Evol. Biosphere.* 28 (1998) 321–347.
- [11] C. S. Cockell, J. Knowland, Ultraviolet radiation screening compounds, *Biol. Rev.* 74 (1999) 311–345.
- [12] R. Losantos, M. S. Churio, D. Sampedro, Computational exploration of the photoprotective potential of Gadusol, *Chemistry Open* 4 (2015) 155 – 160.

- [13] P. T. Grant, C. Middleton, P. A. Planck, R. H. Thomson, The isolation of four aminocyclohexenimines (mycosporines) and a structurally related derivative of cyclohexane-1,3-dione (Gadusol) from the brine shrimp *Artemia*, *Comp. Biochem. Physiol. B.* 80 (1985) 755–759.
- [14] M. J. Bok, M. L. Porter, A. R. Place, T. W. Cronin, Biological sunscreens tune polychromatic ultraviolet vision in mantis shrimp, *Curr. Biol.* 24 (2014) 1636-1642.
- [15] J. Colleter, D. J. Penman, S. Lallement, C. Fauvel, T. Hårebrekke, D. R. Osvik, H. C. Eilertsen, H. D’Cotta, B. Chatain, S. Peruzzi, Genetic inoculation of European Sea bass (*Dicentrarchus labrax L.*) eggs using UV-Irradiation: Observations and perspectives, *PLoS ONE* 9 (2014) 1-11.
- [16] W. C. Dunlap, D. McB. Williams, B. E. Chalker, A. T. Banaszak, Biochemical photoadaptation in vision: UV absorbing pigments in fish eye tissues, *Comp. Biochem. Physiol. B* 93 (1989) 601-607.
- [17] A. Thorpe, R. H. Douglas, F. J. Truscott, Spectral transmission and short-wave absorbing pigments in the fish lens-I. Phylogenetic distribution and identity, *Vision Res.* 33 (1993) 289-300.
- [18] P. Nelson, S. Kojima, G. Losey, Exposure to solar radiation may increase ocular UV-filtering in the juvenile scalloped hammerhead shark, *Sphyrna lewii*, *Marine Biol.* 142 (2003) 53-56.
- [19] M. J. Doughty, A. P. Cullen, C. A. Monteith-McMaster, Aqueous humour and crystalline lens changes associated with ultraviolet radiation or mechanical damage to corneal epithelium in freshwater rainbow trout eyes, *J. Photochem. Photobiol. B* 41 (1997) 165-172.

- [20] H-U. Dahmsa, J-S. Lee, UV radiation in marine ectotherms: Molecular effects and responses, *Aquatic Toxicol.* 97 (2010)3-14.
- [21] A. R. Osborn, K. H. Almabruk, G. Holzwarth, S. Asamizu, J. LaDu, K. M. Kean, P. A. Karplus, R. L. Tanguay, A. T. Bakalinsky, T. Mahmud, De novo synthesis of a sunscreen compound in vertebrates, *eLife* 4 (2015) 1-15.
- [22] A. R. Osborn, T. Mahmud, Interkingdom genetic mix-and-match to produce novel sunscreens, *ACS Synth. Biol.* 11 (2019) 2464–2471.
- [23] J. M. Woolley, M. Staniforth, M. D. Horbury, G. W. Pickings, M. Wills, V. G. Stavros, Unravelling the photoprotection properties of mycosporine amino acid motifs, *J. Phys. Chem. Lett.* 9 (2018) 3043–3048.
- [24] R. Losantos, I. Funes-Ardoiz, J. Aguilera, F. Herrera-Ceballos, C. García-Iriepa, P. J. Campos, D. Sampedro, Rational design and synthesis of efficient sunscreens to boost the solar protection factor. *Angew. Chem. Int. Ed.* 56 (2017) 1–5.
- [25] H. W. Lim, M-I. Arellano-Mendoza, F. Stengel, Current challenges in photoprotection. *J. Am. Acad. Dermatol.* 76 (2017) 91-99.
- [26] J. Krutmann, T. Passeron, Y. Gilaberte, C. Granger, G. Leone, M. Narda, S. Schalka, C. Trullas, P. Masson, H. W. Lim, Photoprotection of the future: challenges and opportunities, *J. Eur. Acad. Dermatol. Venereol.* 34 (2020) 447-454.
- [27] W. C. Dunlap, Y. Yamamoto, Small-molecule antioxidants in marine organisms: antioxidant activity of mycosporine-glycine, *Comp. Biochem Physiol. B* 112 (1995) 105–114.
- [28] E. M. Arbeloa, M. J. Uez, S. G. Bertolotti, M. S. Churio, Antioxidant activity of Gadusol and occurrence in fish roes from Argentine Sea, *Food Chem.* 119 (2010) 586–591.

- [29] H-J. Suh, H-W. Lee, J. Jung, Singlet oxygen quenching by deoxygadusol and related mycosporine-like amino acids from phytoplankton *Prorocentrummicans*, *J. Photosci.* 11 (2004) 77–81.
- [30] K. Kalyanasundaram, *Photochemistry in microheterogeneous systems*, Academic Press Inc. Orlando, 1987.
- [31] S. G. Bertolotti, N. A. Garcia, G. A. Argüello, Effect of the peptide bond on the singlet molecular oxygen mediated sensitized photo-oxidation of tyrosine and tryptophan dipeptides. A kinetic study, *J. Photochem. Photobiol. B* 10 (1991) 57-70.
- [32] C. S. Foote, Definition of type I and type II photosensitized oxidation, *Photochem. Photobiol.* 54 (1991) 659.
- [33] M. S. Baptista, J. Cadet, P. Di Mascio, A. A. Ghogare, A. Greer, M. R. Hamblin, C. Lorente, S. L. Nunez, M. S. Ribeiro, A. H. Thomas, M. Vignoni, T. M. Yoshimura, Type I and type II photosensitized oxidation reactions: guidelines and mechanistic pathways, *Photochem. Photobiol.* 93 (2017) 912-919.
- [34] F. E. Scully, J. Hoigne, Rate constants for reactions of singlet oxygen with phenols and other compounds in water, *Chemosphere* 16 (1987) 681–694.
- [35] R. C. Schmitt, C. Tanielian, R. Dunsbach, C. Wolff, Phenalenone, a universal reference compound for the determination of quantum yields of singlet oxygen $O_2(^1\Delta_g)$ sensitization, *J. Photochem. Photobiol. A* 79 (1994) 11–17.
- [36] N. A. Kuznetsova, E. V. Pykhtina, L. A. Ulanova, O. L. Kaliya, Type-I and type-II photoprocesses in the system photosensitizer–ascorbic acid, *J. Photochem. Photobiol. A* 167, (2004) 37–47.

- [37] R. H. Bisby, C. G. Morgan, I. Hamblett, A. A. Gorman, Quenching of singlet oxygen by Trolox C, ascorbate, and amino acids: Effects of pH and temperature, *J. Phys. Chem. A*. 103 (1999) 7454–7459.
- [38] H-J. Suh, H-W. Lee, J. Jung, Mycosporine glycine protects biological systems against photodynamic damage by quenching singlet oxygen with a high efficiency, *Photochem. Photobiol.* 78 (2003) 109–113.
- [39] M. Moliné, E. M. Arbeloa, M. R. Flores, D. Libkind, M. E. Farías, S. G. Bertolotti, M. S. Churio, M. R. van Broock, UVB photoprotective role of mycosporines in yeast: Photostability and antioxidant activity of mycosporine-gutaminol-glucoside, *Radiat. Res.* 175 (2011) 44–50.
- [40] C. Tournaire, S. Croux, M-T. Mauret, J. Beck, M. Hocquaux, A. M. Braun, E. Oliveros, Antioxidant activity of flavonoids: Efficiency of singlet oxygen ($^1\Delta_g$) quenching. *J. Photochem. Photobiol. B* 19 (1993) 205–215.
- [41] F. Amat-Guerri, M. M. C. López-González, R. Martínez-Utrilla, R. Sastre, Singlet oxygen photogeneration by ionized and un-ionized derivatives of rose bengal and eosin-Y in diluted solutions, *J. Photochem. Photobiol. A* 53 (1990) 199–210.
- [42] M. A. J. Rodgers, P. T. Snowden, Lifetime of $O_2(^1\Delta_g)$ in liquid water as determined by time-resolved infrared luminescence measurements, *J. Am. Chem. Soc.* 104 (1982) 5541-5543.
- [43] A. A. Gorman, M. A. J. Rodgers, in: *CRC Handbook of organic photochemistry*, J. C. Scaiano (Ed.), Singlet oxygen, CRC Press, 1989, pp. 229–247.

- [44] A. H. Thomas, M. P. Serrano, V. Rahal, P. Vicendo, C. Claparols, E. Oliveros, C. Lorente, Tryptophan oxidation photosensitized by pterin, *Free Radical Biol. Med.* 63 (2013) 467–475.
- [45] S. Sharifian, A. Homaei, E. Kamrani, T. Etzerodt, S. Patel, New insights on the marine cytochrome P450 enzymes and their biotechnological importance, *Int. J. Biol. Macromol.* 142 (2020) 811–821.
- [46] S. Criado, J. P. Escalada, A. Pajares, N. A. Garcia, Singlet oxygen [$O_2(^1\Delta_g)$]-mediated photodegradation of tyrosine derivatives in the presence of cationic and neutral micellar systems, *Amino Acids* 35 (2008) 201-208.
- [47] D. E. Orallo, S. G. Bertolotti, M. S. Churio, Photophysical characterization of mycosporine-like amino acids in micellar solutions. *Photochem. Photobiol. Sci.* 16 (2017) 1117–1125.
- [48] A. Posadaz, N. M. Correa, M. A. Biasutti, N. A. García, A kinetic study of the photodynamic effect on tryptophan methyl ester and tryptophan octyl ester in DOPC vesicles. *Photochem. Photobiol.* 86 (2010) 96-103.
- [49] M. Romero, B. Rotondo, J. Mella-Raipán, C. D. Pessoa-Mahana, E. Lissi, C. López-Alarcón, Antioxidant capacity of pure compounds and complex mixtures evaluated by the ORAC-pyrogallol red assay in the presence of Triton X-100 micelles, *Molec.* 15 (2010) 6152-6167.
- [50] E. A. Lissi, M. V. Encinas, E. Lemp, M. A. Rubio, Singlet oxygen $O_2(^1\Delta_g)$, bimolecular processes. Solvent and compartmentalization effects, *Chem. Rev.* 93 (1983) 699-723.

[51] L. Musbat, H. Weitman, B. Ehrenberg, Azide quenching of singlet oxygen in suspensions of microenvironments of neutral and surface charged liposomes and micelles, *Photochem. Photobiol.* 89 (2013) 253-258.

Journal Pre-proof

FIGURE CAPTIONS

Fig. 1. a) Acid-base equilibrium connecting the enol form GADH ($\lambda_{\max} = 268$ nm) with the enolate form, GAD ($\lambda_{\max} = 296$ nm). b) Absorption spectra of gadusol in: aqueous solution at pH 2.5 (solid line); phosphate buffer solution pH 5 (dotted line) and phosphate buffer solution pH 8 (dashed line).

Fig. 2. Stern-Volmer plots for the quenching of singlet oxygen phosphorescence by gadusol species in D₂O at pD 5.0 (squares); pD 8.0 (circles); pD 8.0 and 0.1 mol L⁻¹ SDS (triangles). Vertical bars are derived from the uncertainty in the τ_f values (± 2 μ s).

Fig. 3. Pseudo-first order plots for the reactive quenching of $O_2(^1\Delta_g)$ by gadusol species in aqueous solution. a) Substrate consumption: pH 8 –CAL (circles); pH 5 - data from absorption at 296 nm assigned to GAD (triangles up); pH 5 - data from absorption at 268 nm assigned to GADH (triangles down) and by TRP taken as the reference, (squares). b) Oxygen consumption: pH 8 GAD (empty circles) and TRP (empty squares). Dashed lines denote the linear regression of the data.

Fig. 4. Pseudo-first order plots for the reactive quenching of $O_2(^1\Delta_g)$ by GAD at pH 8 in: 0.10 mol L⁻¹ SDS (circles); 0.10 mol L⁻¹ CTAC (triangles) and neat water (squares). Dashed lines denote the linear regression of the data.

Fig. 5. Proposed pathways for the oxidation of GAD by $O_2(^1\Delta_g)$.

FIGURE. 1

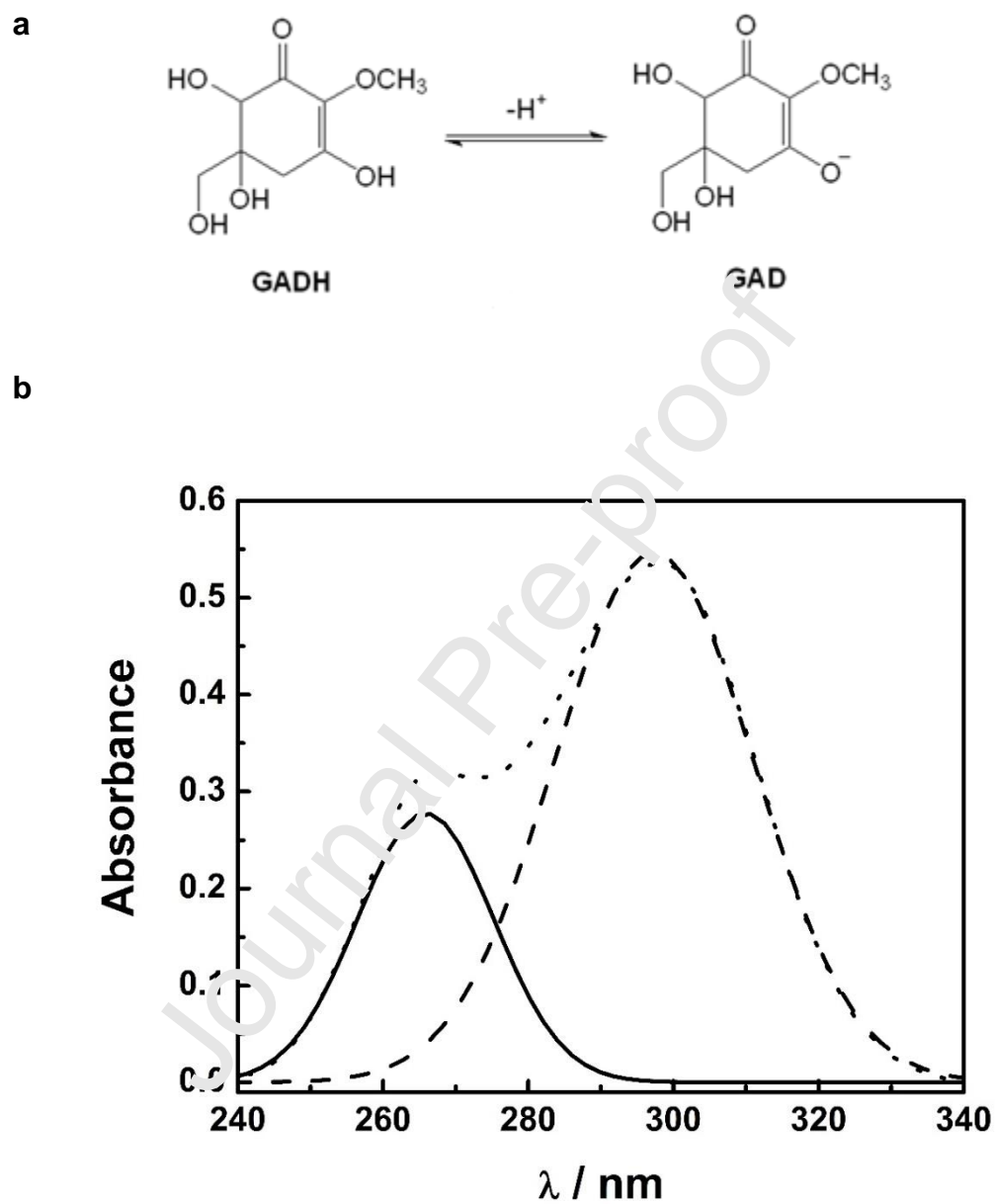


FIGURE 2

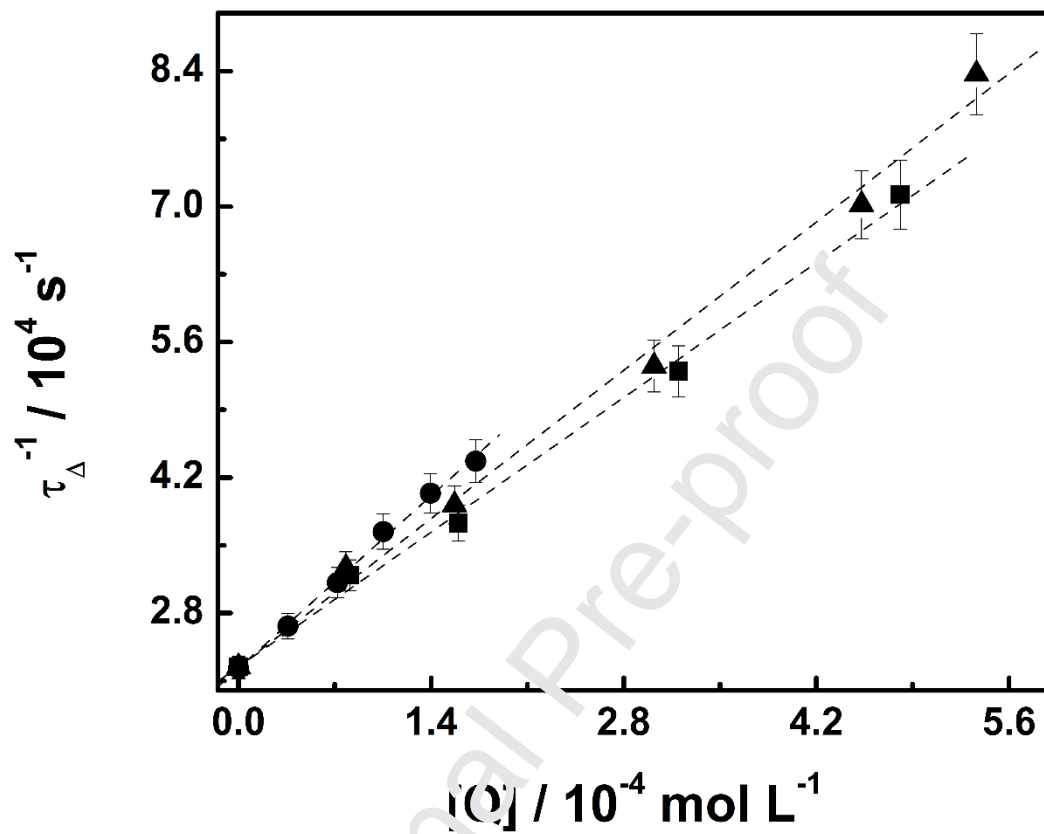


FIGURE 3

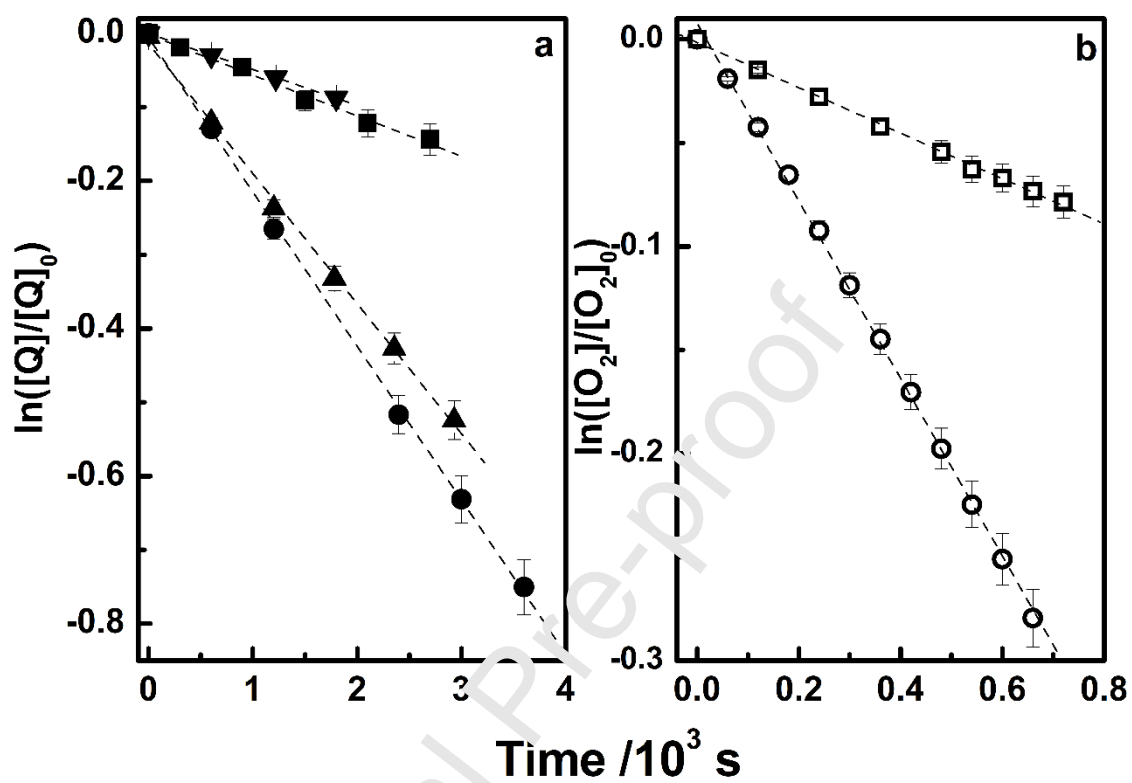


FIGURE 4

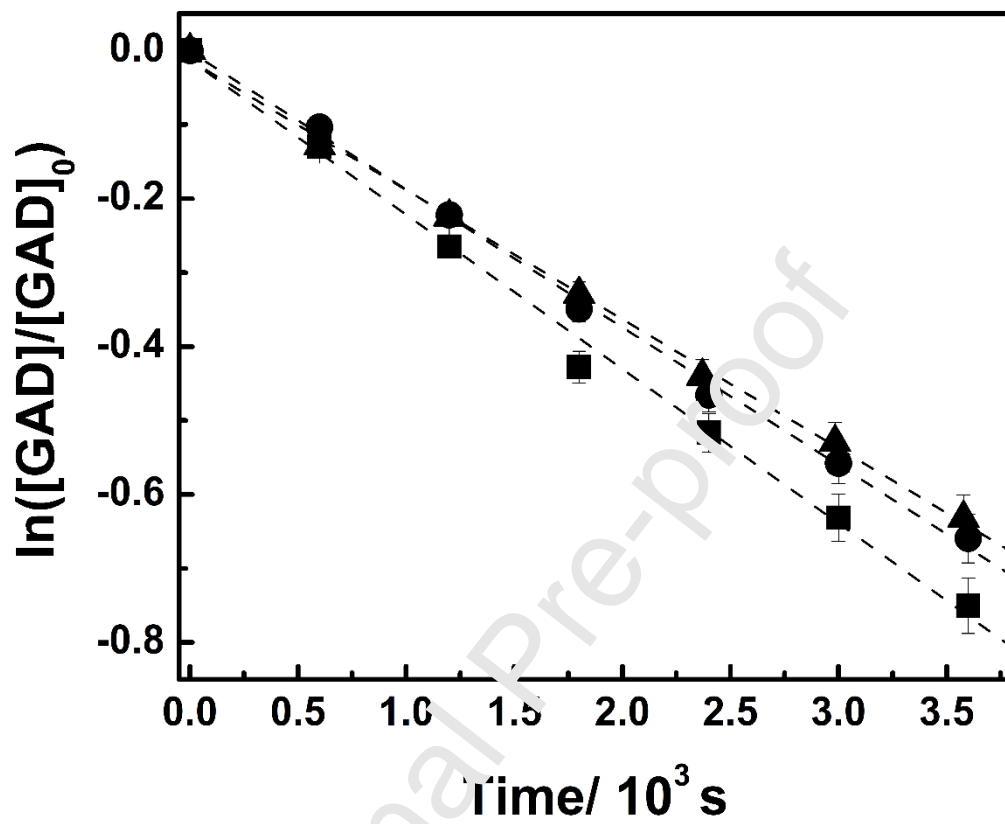


FIGURE 5

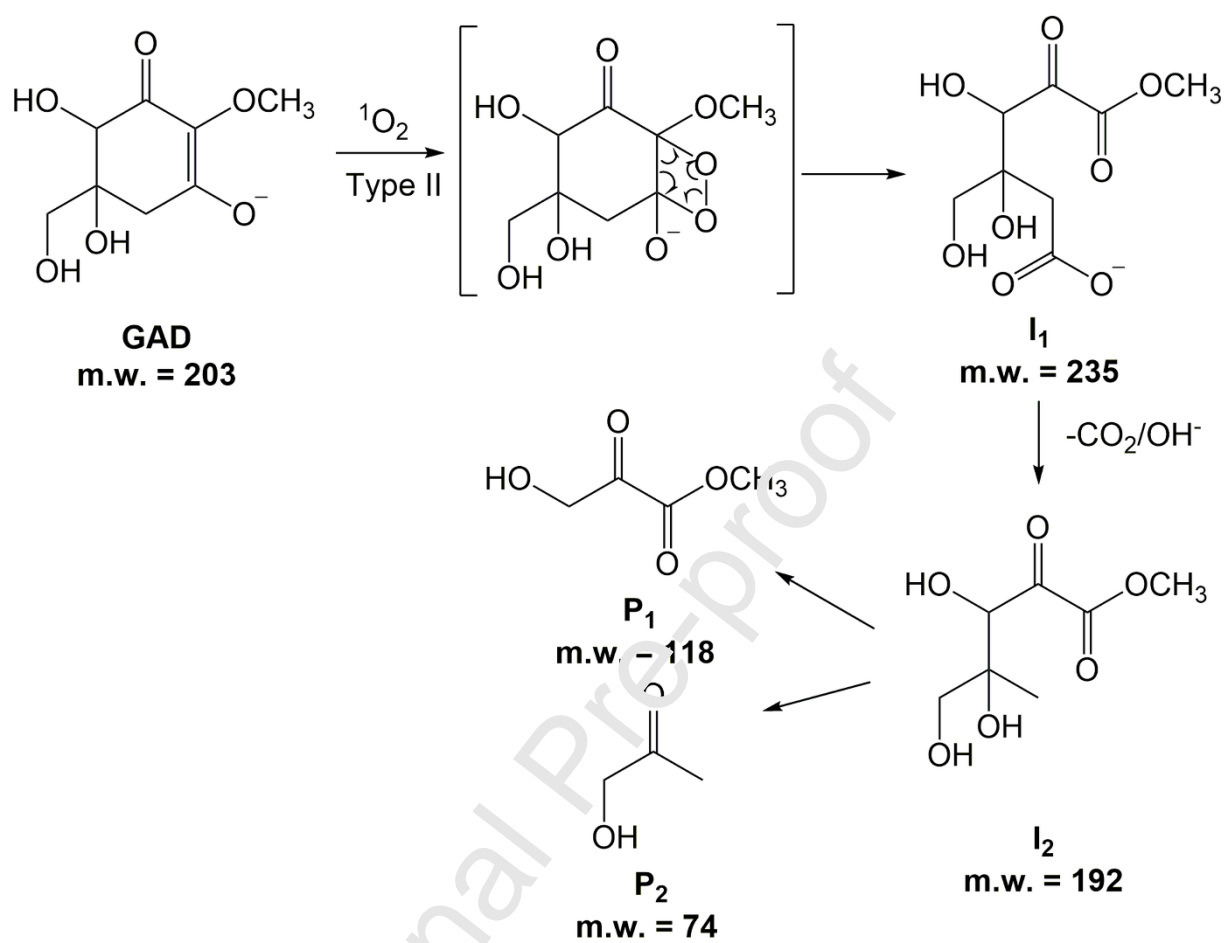


Table 1. Rate constants for the quenching of $O_2(^1\Delta_g)$ by gadusol species in aqueous and micellar solutions

pH (pD)	surfactant	k_t ($10^8 \text{ L mol}^{-1}\text{s}^{-1}$) ^a	k_r ($10^8 \text{ L mol}^{-1}\text{s}^{-1}$) ^b
5.0	-	0.99 ± 0.10	0.18 ± 0.08 ^c
	-		0.93 ± 0.11 ^d
8.0	-	1.27 ± 0.10	1.05 ± 0.19 ^d
	-		0.80 ± 0.10 ^e
	SDS	1.09 ± 0.13 ^f	0.99 ± 0.12 ^{d,f}
	CTAC	1.17 ± 0.17 ^f	1.02 ± 0.11 ^{d,f}

^a Uncertainties in k_t were estimated from the experimental error in τ_{Δ} determined by TRPD

^b Uncertainties in k_r arise from the deviation of at least three independent determinations.

^c Effective constant derived from absorption data at 268 nm (GADH)

^d Effective constant derived from absorption data at 296 nm (GAD)

^e Derived from oxygen consumption

^f Apparent constant

Sensitized photo-oxidation of gadusol species mediated by singlet oxygen

D. E. Orallo et al. JPPB: 2020

HIGHLIGHTS

- Gadusol species deactivate singlet oxygen in aqueous solution.
- Gadusolate, the anionic and biologically relevant form, is *ca.* 700 times more efficient quencher than the neutral species.
- The quenching rates are not affected by the presence of direct charged micelles.
- Photo-oxidation occurs *via* a type II mechanism by the addition of $O_2(^1\Delta_g)$ and subsequent fragmentation of gadusolate.

Mar del Plata, 19th October 2020

Dear Editor

Journal of Photochemistry and Photobiology B: Biology

Below you will find the list of authors of the manuscript entitled: "Sensitized photo-oxidation of gadusol species mediated by singlet oxygen":

- 1) Dalila Elisabet Orallo
- 2) Nayla Jimena Lores
- 3) Ernesto Maximiliano Arbeloa
- 4) Sonia Graciela Bertolotti
- 5) María Sandra Churio*

*corresponding author

Sincerely yours,

A handwritten signature in black ink, appearing to be 'M. S. Churio', written on a light blue background.

Dr. María Sandra Churio*

Declaration of interests

The authors declare that they have no known competing financial interests or personal relationships that could have appeared to influence the work reported in this paper.

The authors declare the following financial interests/personal relationships which may be considered as potential competing interests:

Journal Pre-proof